GENE THERAPY

CRISPR-Cas9 gene repair of hematopoietic stem cells from patients with X-linked chronic granulomatous disease

Suk See De Ravin,[1]*† Linhong Li,[2]* Xiaolin Wu,[3] Uimook Choi,[1] Cornell Allen,[2] Sherry Koontz,[1] Janet Lee,[1] Narda Theobald-Whiting,[1] Jessica Chu,[1] Mary Garofalo,[1] Colin Sweeney,[1] Lela Kardava,[4] Susan Moir,[4] Angelia Viley,[2] Pachai Natarajan,[2] Ling Su,[3] Douglas Kuhns,[1] Kol A. Zarember,[1] Madhusudan V. Peshwa,[2] Harry L. Malech[1]†

Gene repair of CD34$^+$ hematopoietic stem and progenitor cells (HSPCs) may avoid problems associated with gene therapy, such as vector-related mutagenesis and dysregulated transgene expression. We used CRISPR (clustered regularly interspaced short palindromic repeat)/Cas9 (CRISPR-associated 9) to repair a mutation in the *CYBB* gene of CD34$^+$ HSPCs from patients with the immunodeficiency disorder X-linked chronic granulomatous disease (X-CGD). Sequence-confirmed repair of >20% of HSPCs from X-CGD patients restored the function of NADPH (nicotinamide adenine dinucleotide phosphate) oxidase and superoxide radical production in myeloid cells differentiated from these progenitor cells in vitro. Transplant of gene-repaired X-CGD HSPCs into NOD (nonobese diabetic) SCID (severe combined immunodeficient) $\gamma c^{-/-}$ mice resulted in efficient engraftment and production of functional mature human myeloid and lymphoid cells for up to 5 months. Whole-exome sequencing detected no indels outside of the *CYBB* gene after gene correction. CRISPR-mediated gene editing of HSPCs may be applicable to other CGD mutations and other monogenic disorders of the hematopoietic system.

INTRODUCTION

Transplantation of normal hematopoietic stem and progenitor cells (HSPCs) has proved beneficial for treating many genetic diseases of the hematopoietic system. However, allogeneic transplants are complicated by graft-versus-host disease and limited donor availability (*1*). Gene therapy using autologous HSPCs modified by integrating viral vectors has provided clinical benefit but is complicated by vector-related genotoxicities and transgene expression driven by exogenous promoters (*2*–*4*). Recent lentiviral vector gene therapy trials have reported clinical benefits without any insertional mutagenesis (*5*–*7*). Targeted gene editing using CRISPR (clustered regularly interspaced short palindromic repeat)/Cas9 (CRISPR-associated 9) nuclease has great potential as a therapeutic approach for treating monogenic hematological diseases because of the availability of autologous HSPCs (*8*). CRISPR/Cas9, guided by a single-guide RNA, achieves efficient double-stranded DNA breaks (*9*, *10*). The double-stranded DNA breaks undergo repair either by nonhomologous end joining (NHEJ) causing insertions or deletions (indels) or by homology-directed repair (HDR), which allows donor DNA incorporation. The CRISPR/Cas9 system has shown broad applications in targeted gene editing in plants, mice, and cynomolgus monkey embryos (*11*–*14*). Zinc finger nucleases have been used to enhance HDR in human HSPCs, but there has been a poor correlation between HDR correction rates in vitro and observed correction rates in human gene-repaired cells after transplant into immunodeficient NOD (nonobese diabetic) SCID (severe combined immunodeficient) $\gamma c^{-/-}$ (NSG) mice. This suggests that there may exist a barrier to gene modification and subsequent engraftment of CD34$^+$ HSPCs (*15*, *16*).

X-linked chronic granulomatous disease (X-CGD) arises from mutations in *CYBB*, the gene encoding gp91^{phox}, which is the catalytic center of NADPH (nicotinamide adenine dinucleotide phosphate) oxidase 2 (NOX2). NOX2 expressed by phagocytic cells produces superoxide anions that have microbicidal and immunoregulatory functions (*17*). Patients with X-CGD suffer from life-threatening infections and require prophylactic antimicrobial therapy. The amount of residual NOX2 activity in neutrophils from X-CGD patients predicts patient survival, suggesting that small improvements in NOX2 function may provide clinical benefit (*17*). Differing degrees of X chromosome inactivation in female carriers of X-CGD result in a range of disease phenotypes (*18*). In general, increased susceptibility to infections occurs when <10 to 15% of neutrophils are functionally normal, suggesting that restoration of NOX2 to only 10 to 15% of neutrophils would provide clinical benefit in X-CGD. The most frequent mutation occurring in a National Institutes of Health cohort of X-CGD patients (17 of 284; 6%) was the C676T substitution in exon 7 of the *CYBB* gene, resulting in a premature stop codon and an inactive gp91^{phox} protein (*17*). This mutation was therefore chosen for repair using the CRISPR/Cas9/single-guide RNA system. The goal of our study was to achieve efficient repair of this gene mutation in CD34$^+$ HSPCs from X-CGD patients at clinically relevant levels.

[1]Laboratory of Host Defenses, National Institute of Allergy and Infectious Diseases, National Institutes of Health, Bethesda, MD 20892, USA. [2]MaxCyte Inc., Gaithersburg, MD 20878, USA. [3]Cancer Research Technology Program, Leidos Biomedical Research Inc., Frederick, MD 21701, USA. [4]Laboratory of Immunoregulation, National Institutes of Allergy and Infectious Diseases, National Institutes of Health, Bethesda, MD 20892, USA.
*These authors contributed equally to this work.
†Corresponding author. Email: sderavin@niaid.nih.gov (S.S.D.R.); hmalech@nih.gov (H.L.M.)

RESULTS

Optimization of CRISPR-mediated gene repair in patient-derived immortalized B cells

To determine the activity of the CRISPR system directed by a site-specific guide, we used Epstein-Barr virus (EBV)–transformed B cell lines derived from patient 1 (P1) with X-CGD. Four guides targeting

sequences around the *CYBB* C676T site were evaluated, of which single-guide RNA2 displayed maximal cutting efficiency (fig. S1, A to C).

Although both single- and double-stranded DNA fragments have been used to promote HDR-mediated gene repair (*19*, *20*), the former were chosen for this study. Phosphorothioate modifications of a single-stranded oligodeoxynucleotide (ssODN) protect against nuclease degradation, improving activity but possibly at the cost of increasing toxicity to cell lines (*21*, *22*). We evaluated the effects of increasing phosphorothioate modifications in the EBV P1 cell line and observed stable viability and proliferative capabilities, indicating that the modifications were tolerated (fig. S2, A and B). The 2p phosphorothioate modification of the ssODN resulted in the highest rate of gene correction with restored gp91^{phox} expression that was stable for 30 days (fig. S2C). Sequencing of the corrected EBV P1 cell line confirmed genetic repair of the mutation to the normal sequence (fig. S2D), with increasing gene correction inversely related to the number of indels.

Targeting of CRISPR to the *CYBB* 676 locus of normal CD34$^+$ HSPCs

To facilitate the development of gene repair by CRISPR in CD34$^+$ HSPCs from X-CGD patients, we first evaluated the feasibility of the CRISPR/single-guide approach for targeting normal human CD34$^+$ HSPCs. Mobilized CD34$^+$ HSPCs in the peripheral blood of healthy controls were collected and cryopreserved in the same process used for mobilized CD34$^+$ HSPCs from X-CGD patients, with the purity of CD34$^+$ HSPCs being >95% [National Institute of Allergy and Infectious Diseases (NIAID)–approved protocol 94-I-0073]. We applied the same single guide with a base pair difference at nucleotide 676 of the *CYBB* gene, a "C" in healthy donor CD34$^+$ HSPCs instead of the "T" occurring in the subset of X-CGD patients whom we studied. The donor template used in the healthy CD34$^+$ HSPCs carried a single base pair mutation "T" so that a successful HDR event would create the *CYBB* C676T mutation. Given that the successful creation of both the missense mutation and indels would abrogate gp91^{phox} function, the outcome of this system depended on sequencing of the alleles. The various conditions evaluated showed up to 80% gene editing rates (HDR-mediated *CYBB* C676T mutation up to 21% and indels >70%) (Fig. 1A). To evaluate gene editing rates in CD34$^+$ HSPCs, we sorted CRISPR-treated CD34$^+$ HSPCs into various CD34$^+$ subpopulations: primitive (CD34$^+$CD133$^+$CD90$^+$), early (CD34$^+$CD133$^+$CD90$^-$), and committed (CD34$^+$CD133$^-$) progenitor cells and differentiated cells (CD34$^-$). Similar rates of gene editing were observed in all four CD34$^+$ subpopulations in contrast to the reduced levels of gene editing reported previously in more primitive CD34$^+$ subpopulations (Fig. 1A) (*13*). This difference may be partly attributable to different cell sources, with cord blood and bone marrow the source of CD34$^+$ cells used in previous studies compared to the granulocyte colony-stimulating factor (G-CSF)–mobilized peripheral blood CD34$^+$ HSPCs used in our study.

CYBB gene mutation repair in mobilized CD34$^+$ HSPCs from X-CGD patients

Next, we investigated CRISPR-mediated gene repair in mobilized CD34$^+$ HSPCs from X-CGD P1 with the C676T mutation (*23*). We evaluated electroporation conditions including the cell concentration during electroporation, as well as the amounts of Cas9, single-guide RNA, and donor ssODN template required. Cell viability, proliferative capacity, and restoration of gp91^{phox} expression were determined by flow cytometry (FACS) (fig. S3). Of the conditions tested, the best outcomes when considering both correction efficiencies and cell toxicities were achieved with P1 CD34$^+$ HSPCs at 3×10^7 to 6×10^7/ml with Cas9 at 100 μg/ml, single-guide RNA at 200 to 300 μg/ml, and ssODN at 100 to 200 μg/ml (Figs. 1 to 4 and fig. S3).

Notably, this seamless repair of a missense mutation in situ restored gene function, with expression under the control of the gene's endogenous promoter rather than an exogenous promoter. Consequently, given that CD34$^+$ HSPCs do not normally express gp91^{phox}, differentiation of the corrected CD34$^+$ HSPCs into myeloid cells was required to assess restoration of gene expression and function. Using optimized conditions, we cultured corrected P1 CD34$^+$ HSPCs for 2 to 3 weeks in vitro to induce myeloid differentiation. Thirty-one percent of the corrected CD34$^+$ HSPC–derived myeloid cells showed gp91^{phox} expression compared to 95% of myeloid cells derived from uncorrected healthy control CD34$^+$ HSPCs (Fig. 1B). NOX2 activity was first evaluated using the DHR assay, which measures the production of reactive oxygen species (ROS) by FACS after PMA stimulation of myeloid cells. After myeloid differentiation of corrected P1 CD34$^+$ HSPCs, 19.3% of myeloid cells were positive for NOX2 activity compared to <0.1% of uncorrected naïve patient myeloid cells and 80% of healthy control myeloid cells (Fig. 1C). Superoxide radical production after PMA stimulation of myeloid cells was measured by luminol-enhanced chemiluminescence. Superoxide radical production from myeloid cells derived from corrected P1 CD34$^+$ HSPCs was about one-third of the amount produced by normal healthy control myeloid cells (Fig. 1D).

To determine the antibacterial activity of gene-repaired myeloid cells, corrected P1 myeloid cells derived from CD34$^+$ HSPCs were incubated with *G. bethesdensis*, a Gram-negative bacterium first identified as a human pathogen in CGD patients (*24*). Corrected P1 myeloid cells showed a trend toward improved antimicrobial activity, indicated by a reduction in bacterial colony counts in two independent experiments (Fig. 1E).

Transplantation of corrected P1 CD34$^+$ HSPCs into NSG immunodeficient mice

We next evaluated whether CRISPR-repaired P1 CD34$^+$ HSPCs maintained in vivo repopulating capacity after transplantation into immunodeficient NSG mice. After optimization, except where indicated, all experiments were performed with Cas9 nuclease (100 μg/ml) and single-guide RNA (200 μg/ml), with varying doses of ssODN ranging from 40 to 300 μg/ml (to determine the potential long-term consequences of the amount of donor template used). Gene-corrected or uncorrected P1 CD34$^+$ HSPCs or healthy control CD34$^+$ HSPCs were transplanted into 6- to 8-week-old NSG mice (n = 3 independent experiments, n = 36 mice total). Cells were also cultured in vitro and showed repair rates of 12 to 31%, as indicated by gp91^{phox} expression depending on the amount of ssODN (Figs. 1C and 3, C and D). Gene correction outcomes were determined in mouse peripheral blood (Fig. 2) and bone marrow (Fig. 3) at 8, 16, or 20 weeks after transplant of CD34$^+$ HSPCs into NSG mice. Human myeloid cells derived from transplanted CD34$^+$ HSPCs were identified in mouse peripheral blood by FACS staining for human CD45$^+$ and gp91^{phox} expression (Fig. 2A). HSPC-derived myeloid cells in mouse peripheral blood after correction with ssODN (200 μg/ml) were 21.1 ± 9.8% of total (three independent experiments, means ± SD, n = 9 mice) (Fig. 2B). Of these, 15.6 ± 3.5% (n = 9 mice) expressed gp91^{phox} compared with 65.6% of human myeloid cells derived from healthy control HSPCs

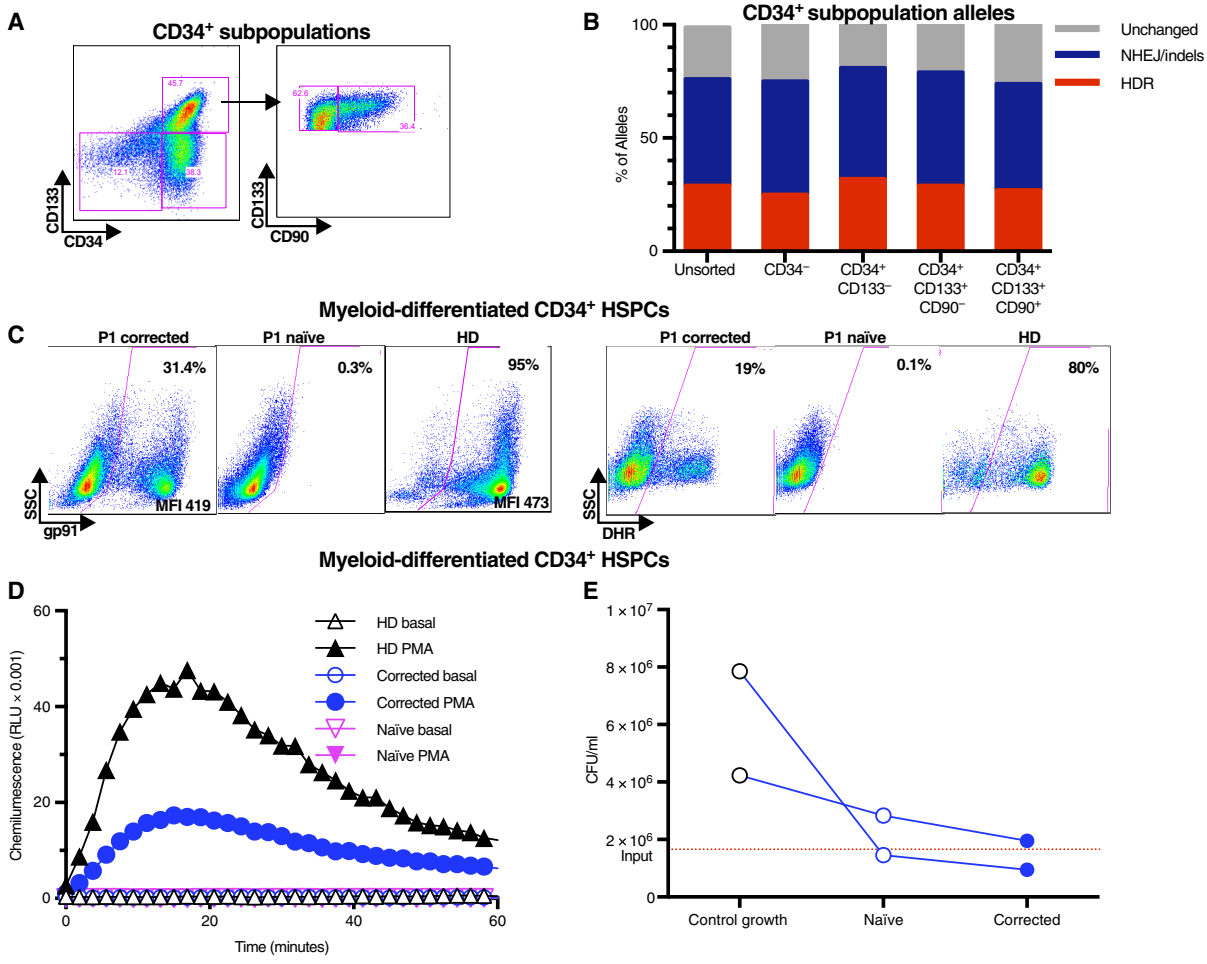

Fig. 1. CRISPR-mediated correction of CD34$^+$ HSPCs from a patient with X-CGD. (**A**) Gene editing rates in mobilized CD34$^+$ HSPC subpopulations in peripheral blood from a healthy control donor. Fluorescence-activated cell sorting (FACS) strategy for sorting cells into primitive (CD34$^+$CD133$^+$CD90$^+$), early (CD34$^+$CD133$^+$CD90$^-$), and committed (CD34$^+$CD133$^-$) progenitor cells and differentiated myeloid cells (CD34$^-$). Comparison of rates of alleles representing unchanged sequence, indels due to NHEJ, and repaired mutations after HDR in unsorted and FACS-sorted CD34$^+$ HSPC subpopulations. (**B**) gp91^{phox} expression assessed by FACS analysis [mean fluorescence intensity (MFI)] of gene-corrected and uncorrected (naïve) myeloid cells differentiated from P1 CD34$^+$ HSPCs and healthy control CD34$^+$ HSPCs. (**C**) NOX2 activity after phorbol 12-myristate 13-acetate (PMA) stimulation assessed by the dihydrorhodamine (DHR) assay for gene-corrected and uncorrected (naïve) myeloid cells differentiated from P1 and healthy control CD34$^+$ HSPCs. SSC, side scatter. (**D**) Luminol-enhanced chemiluminescence for detecting superoxide radical production by myeloid cells derived from gene-corrected P1 (corrected) or uncorrected P1 (naïve) CD34$^+$ HSPCs from P1 or healthy control HSPCs (HD). Relative light units (RLU) are shown on the *y* axis. (**E**) Antibacterial activity of myeloid cells derived from gene-corrected P1 (corrected) or uncorrected P1 (naïve) CD34$^+$ HSPCs. Myeloid cells were incubated with *Granulibacter bethesdensis* (concentration of bacteria added is indicated by dotted lines) at a multiplicity of infection (MOI) of 1 for 24 hours, and colony-forming units (CFU) were enumerated (results of two independent experiments are plotted).

in mouse peripheral blood (Fig. 2B). Among the gene-corrected groups, a difference was observed in the percentage of human CD45$^+$ cells in mouse peripheral blood only in the 80 versus 40 μg ssODN/ml groups (adjusted P = 0.01) and the 80 versus 300 μg ssODN/ml groups (adjusted P = 0.04, Tukey's multiple comparisons test) (Fig. 2B). The uncorrected groups were not compared because an unequal number of CD34$^+$ HSPCs were transplanted. With respect to human CD45$^+$ myeloid cells expressing gp91^{phox} in mouse peripheral blood, a difference was observed when comparing 40 and 200 μg ssODN/ml groups (adjusted P = 0.002), 40 to 300 μg ssODN/ml groups (adjusted P = 0.018), and 80 versus 200 μg ssODN/ml groups (adjusted P = 0.02, Tukey's multiple comparisons test) (Fig. 2C). The amount of gp91^{phox} expressed by P1 gene-repaired myeloid cells in mouse peripheral blood was comparable to that of healthy control myeloid cells (Fig. 2D). Superoxide radical production by corrected CD45$^+$ human myeloid cells in mouse peripheral blood was about one-third that of healthy control myeloid cells (Fig. 2E).

Although NOX2 is primarily associated with myeloid cell function, alterations in NOX2 activity in B lymphocytes have also been reported in CGD patients (*25*, *26*). We evaluated gp91^{phox} expression in human CD45$^+$ cells by FACS in mouse peripheral blood after transplantation of corrected or uncorrected P1 or healthy control CD34$^+$ HSPCs. The forward scatter– and side scatter–gated lymphocyte subset contained ~32% CD20$^+$ B cells compared to <1% in the granulocyte-gated population (Fig. 3A). Using this gating strategy, we assessed gp91^{phox} expression in lymphocyte subsets in mouse peripheral blood at 20 weeks after transplant. About 7% of human CD20$^+$ B cells from corrected P1 CD34$^+$ HSPCs expressed gp91^{phox} compared to 19% of healthy control

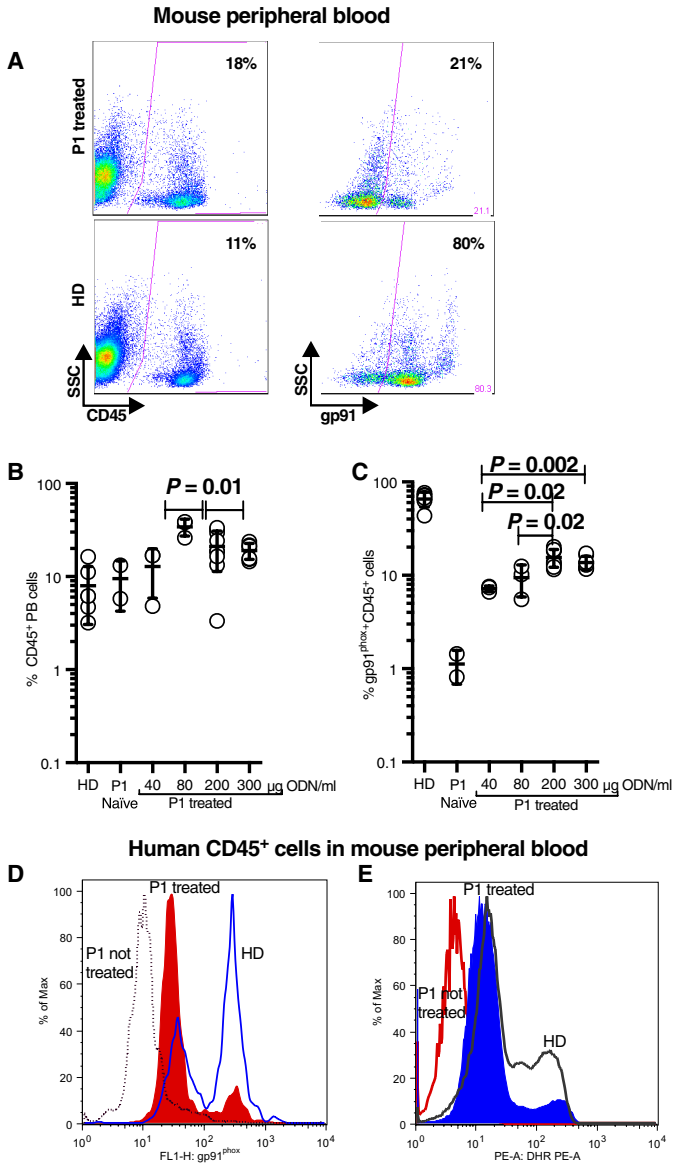

Fig. 2. Gene-corrected patient cells in mouse peripheral blood after transplant of CD34$^+$ HSPCs. (**A**) Representative FACS analysis showing the strategy for evaluating engraftment of CD34$^+$ HSPCs after transplant into NSG mice. The number of human CD45$^+$ cells in mouse peripheral blood expressing gp91^{phox} was assessed 20 weeks after transplant of corrected or uncorrected (naïve) P1 CD34$^+$ HSPCs or healthy control CD34$^+$ HSPCs. Human CD45$^+$ cells (left) were gated by FACS and analyzed for gp91^{phox} expression (right). (**B** and **C**) Percentage of human CD45$^+$ cells (B) and percentage of human CD45$^+$ cells expressing gp91^{phox} (C) in mouse peripheral blood after transplant of P1 CD34$^+$ HSPCs either uncorrected or corrected with varying amounts of ssODN as indicated. Significant differences in percentage of human CD45$^+$ cells were observed in the 80 versus 40 µg ssODN/ml groups (adjusted $P = 0.01$) and the 80 versus 300 µg ssODN/ml groups (adjusted $P = 0.04$) (B). For human CD45$^+$gp91^{phox}-expressing cells in mouse peripheral blood (PB), a difference was observed when comparing 40 and 200 µg ssODN/ml groups (adjusted $P = 0.002$), 40 to 300 µg ssODN/ml groups (adjusted $P = 0.018$), and 80 versus 200 µg ssODN/ml groups (adjusted $P = 0.02$). Data are from three independent experiments, means ± SD, Tukey's multiple comparisons test. (**D**) Representative histogram of FACS analysis of gp91^{phox} protein expression in gene-corrected (red) and uncorrected naïve (black dotted line) P1 and healthy control donor (HD; blue) CD34$^+$ HSPCs after transplant. (**E**) NOX2 activity measured by the DHR assay in mouse peripheral blood after transplant with P1 corrected (blue) or uncorrected naïve (red) CD34$^+$ HSPCs or healthy control donor CD34$^+$ HSPCs (black).

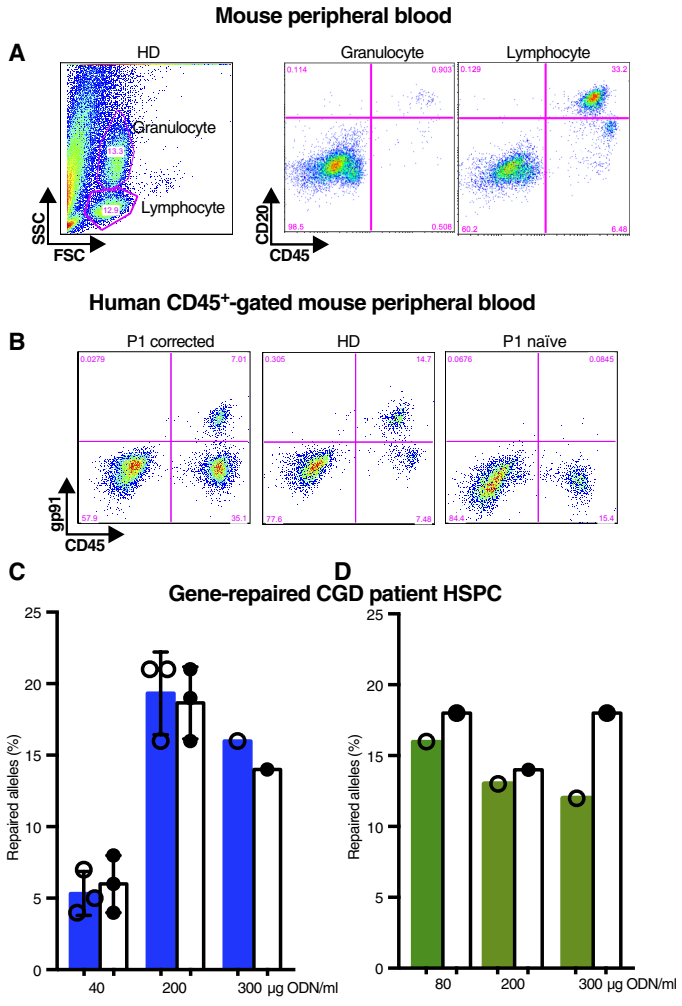

Fig. 3. Expression of gp91^{phox} by human B lymphocytes in mouse peripheral blood after transplant. (**A**) FACS analysis of mouse peripheral blood after transplant with corrected or uncorrected (naïve) P1 CD34$^+$ HSPCs or healthy control donor CD34$^+$ HSPCs. Granulocyte (top) and lymphocyte (bottom) gates were set with forward and side scatter for the healthy control donor (HD) cells. The lymphocyte-gated population contained predominantly CD45$^+$CD20$^+$ human B cells. (**B**) Expression of gp91^{phox} in lymphocyte-gated human cells in mouse peripheral blood after transplant with corrected or uncorrected (naïve) P1 CD34$^+$ HSPCs or healthy control donor (HD) CD34$^+$ HSPCs. (**C** and **D**) Percentage of repaired alleles in gene-corrected P1 CD34$^+$ HSPCs and healthy control CD34$^+$ HSPCs (with ODN amounts as indicated) was determined before transplant (green bars) and after 3 to 4 weeks of differentiation into myeloid cells in vitro (white bars). Human CD45$^+$ cells in mouse bone marrow after transplant of gene-corrected P1 CD34$^+$ HSPCs or healthy control CD34$^+$ HSPCs were also sequenced at harvest (blue bars) and after 3 to 4 weeks of in vitro culture (white bars).

B cells (Fig. 3B). The utility of FACS evaluation of gp91^{phox} expression by CD3$^+$ T cells was limited given that this protein is not normally expressed in CD3$^+$ T cells (fig. S4).

To address the question of whether gene-repaired P1 CD34$^+$ HSPCs could have a survival advantage, we compared the frequencies of gene-corrected alleles in human CD45$^+$ cells in mouse bone marrow before and after 3 weeks of culture (Fig. 3C). The same comparison was performed on gene-repaired P1 CD34$^+$ HSPCs before and after 3 to 4 weeks of myeloid differentiation in vitro (Fig. 3D). The data confirmed stability of gene repair and showed no survival

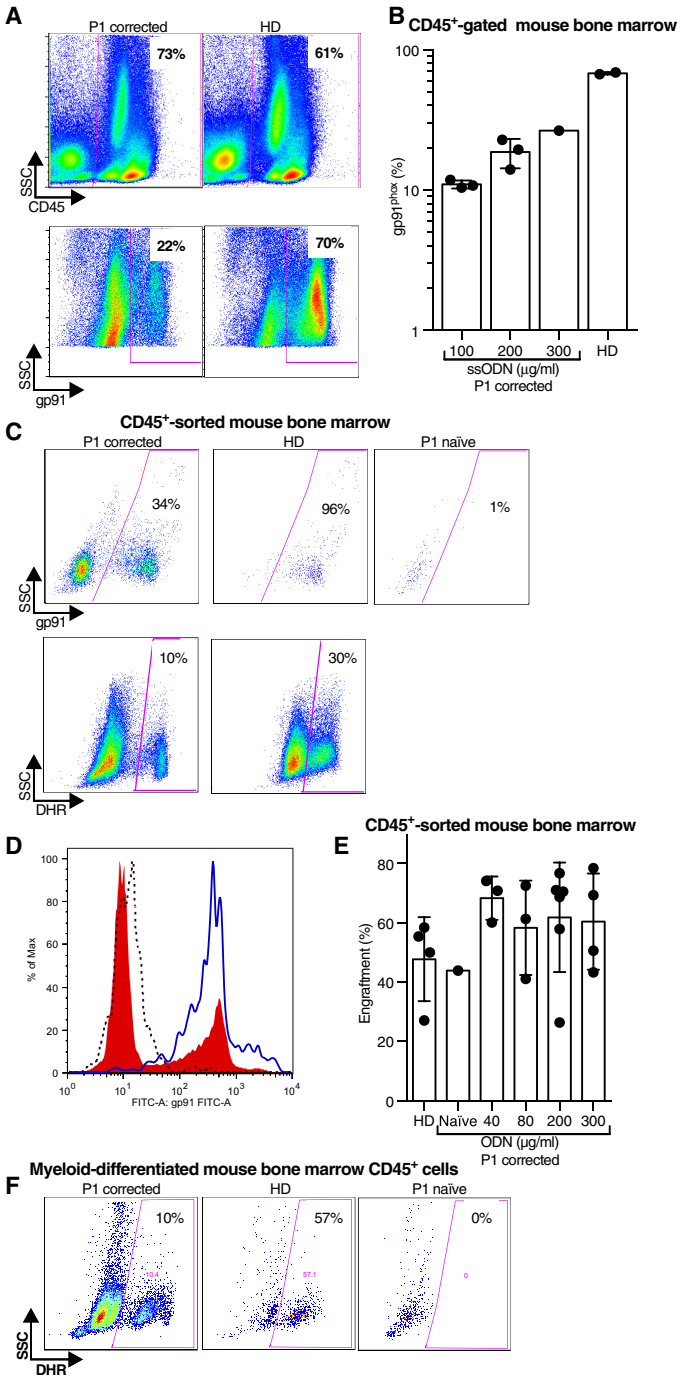

Fig. 4. Analysis of mouse bone marrow after transplant of corrected patient or control CD34$^+$ HSPCs. (**A**) Representative FACS analysis of human CD45$^+$ cells in mouse bone marrow at 8 weeks after transplant (top) and gp91^{phox} expression (bottom) by human CD45$^+$ cells derived from gene-corrected or uncorrected (naïve) P1 CD34$^+$ HSPCs or healthy control donor (HD) CD34$^+$ HSPCs. (**B**) Effects of increasing ssODN dose (μg/ml) on the percentage of human CD45$^+$ cells expressing gp91^{phox} in mouse bone marrow after transplant. (**C**) Mouse bone marrow 20 weeks after transplant was sorted for human CD45$^+$ myeloid cells derived from P1 corrected or uncorrected (naïve) or healthy control donor (HD) CD34$^+$ HSPCs and stained for gp91^{phox} expression or NOX2 activity assessed by the DHR assay. (**D**) FACS analysis of gp91^{phox} expression shown in (C), depicted as a histogram. Gene-corrected P1 cells (red) or uncorrected (naïve) P1 cells (black dotted line) or healthy control donor cells (HD; blue line). FITC, fluorescein isothiocyanate. (**E**) Engraftment rates in mouse bone marrow for CD34$^+$ HSPCs from P1 corrected with different concentrations of ssODN (μg/ml). Columns show means ± SD; each mouse received 1 million to 3 million corrected P1 CD34$^+$ HSPCs. (**F**) NOX2 activity in human CD45$^+$ cells sorted from mouse bone marrow was determined using the DHR assay after transplant of NSG mice with P1 corrected or uncorrected (naïve) CD34$^+$ HSPCs or healthy control donor (HD) CD34$^+$ HSPCs.

advantage for gene-repaired myeloid cells (Fig. 3, C and D). Previous transplant and gene therapy trials have reported a competitive survival disadvantage for HSPCs transduced with a gp91^{phox}-expressing viral vector (*27*).

We then analyzed mouse bone marrow at 6 to 8, 16, or 20 weeks after transplant for human CD45$^+$ cells by FACS (Fig. 4A). There was >60 ± 14.8% (means ± SD, n = 16 mice) human CD45$^+$ cells derived from engrafted gene-repaired P1 CD34$^+$ HSPCs at 8 weeks after transplant in mouse bone marrow. There was 16.5 ± 6.4% (n = 7) human CD45$^+$ cells derived from gene-repaired P1 CD34$^+$ HSPCs expressing gp91^{phox} compared to 67% of human CD45$^+$ cells derived from healthy control CD34$^+$ HSPCs in mouse bone marrow (Fig. 4A). The rates of correction trended higher with increasing amounts of ssODN but did not reach statistical significance, possibly related to the small sample size (Fig. 4B). At 20 weeks after transplant, FACS-sorted human CD45$^+$ cells from gene-repaired P1 CD34$^+$ HSPCs in mouse bone marrow that were cultured for 7 days with G-CSF to promote myeloid maturation demonstrated about one-third the amount of gp91^{phox} expression as human CD45$^+$ cells derived from healthy control CD34$^+$ HSPCs (Fig. 4C). The MFI of gp91^{phox} expression by FACS was similar for myeloid cells from gene-repaired P1 and healthy control CD34$^+$ HSPCs, as expected given the endogenous regulation of *CYBB* (Fig. 4D). Furthermore, the engraftment rates for gene-repaired P1 CD34$^+$ HSPCs treated with different amounts of ssODN were similar (Fig. 4E). Functional NOX2 activity measured by the DHR assay in human CD45$^+$ cells derived from corrected P1 CD34$^+$ HSPCs in mouse bone marrow was one-third that of human CD45$^+$ cells from healthy control CD34$^+$ HSPCs (Fig. 4F). The same CRISPR-mediated gene correction with similar amounts of ssODN was applied to CD34$^+$ HSPCs from a second X-CGD patient with the same mutation; similar results were obtained regarding *CYBB* mutation correction, restoration of gp91^{phox} expression, and NOX2 activity (figs. S6 and S7).

Persistence of gene repair after transplant of corrected P1 CD34$^+$ HSPCs into NSG mice

Concerns about gene-edited CD34$^+$ HSPCs include whether the true repopulating CD34$^+$ HSPCs are corrected and whether treatment-associated toxicities could inhibit either engraftment or long-term correction (*15*, *16*). To address these issues, we compared data from in vitro cultures or mouse peripheral blood taken 6 or 20 weeks after transplant of CD34$^+$ HSPCs. There were 62.6 ± 14.8% human CD45$^+$ cells in mouse bone marrow at 8 weeks after transplant and 61.6 ± 13.3% at 20 weeks after transplant (n = 9) (Fig. 5A). In mouse peripheral blood, human CD45$^+$ myeloid cells derived from gene-corrected P1 CD34$^+$ HSPCs showed 14% stable expression of gp91^{phox}, with no significant decline in expression from 6 to 20 weeks after transplant (Fig. 5B). We then compared rates of gene correction between in vitro gene-corrected P1 CD34$^+$HSPCs and human CD45$^+$ cells derived from transplanted gene-corrected P1 CD34$^+$ HSPCs at 8, 16, or 20 weeks after transplant (Fig. 5C). Deep sequencing of the

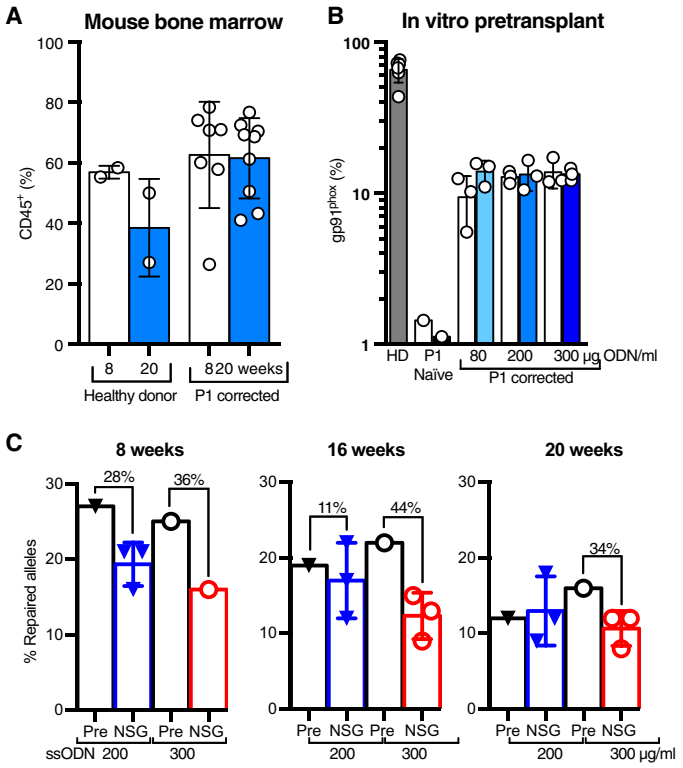

Fig. 5. Long-term persistence of engrafted cells and repaired alleles after transplant of patient CD34$^+$ HSPCs. (**A**) Human CD45$^+$ myeloid cells in mouse peripheral blood at 8 or 20 weeks after transplant with corrected or uncorrected (naïve) P1 or healthy control donor (HD) CD34$^+$ HSPCs. Columns represent means ± SD of all animals (pooled, $n = 3$ experiments). (**B**) Percent of human CD45$^+$ myeloid cells in mouse peripheral blood expressing gp91^{phox+} after transplant with corrected or uncorrected (naïve) P1 or healthy control donor (HD) CD34$^+$ HSPCs. The doses of ssODN used for gene correction are shown. White bars, 6 to 8 weeks after transplant; colored bars, 20 weeks after transplant. (**C**) CRISPR-corrected *CYBB* alleles in P1 CD34$^+$ HSPCs before transplant (Pre; white bars) and in sorted human CD45$^+$ cells from mouse bone marrow (NSG) at 8, 16, or 20 weeks after transplant with P1 CD34$^+$ HSPCs corrected with ssODN at either 200 µg/ml (blue) or 300 µg/ml (red).

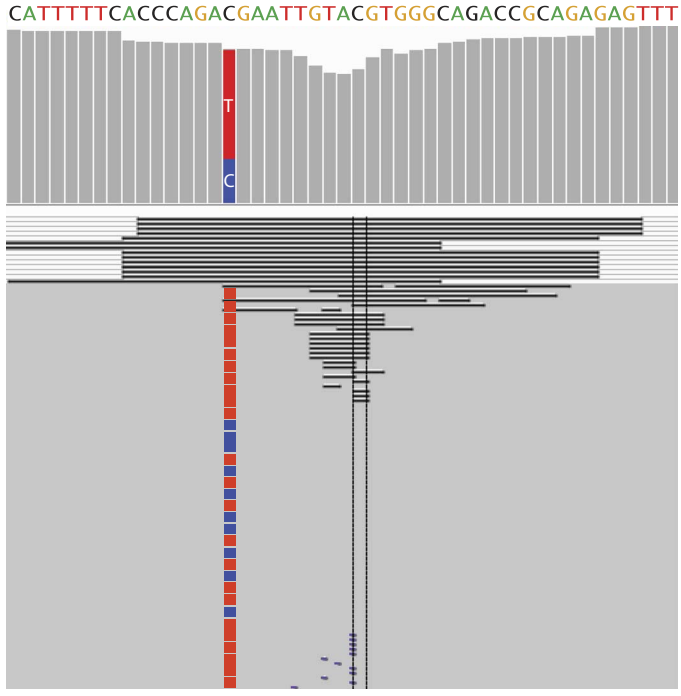

Fig. 6. Deep sequencing of the *CYBB* locus in corrected patient CD34$^+$ HSPCs. Integrated genomics view of the C676T mutation after CRISPR/Cas9 correction was determined by targeted sequencing of the *CYBB* locus. (**Top**) Frequency of the mutant allele (T; red), repaired allele (C; blue), and the coverage depth around the CRISPR cutting site. The dip represents the indels around the CRISPR cutting site. (**Bottom**) Typical allele distribution from a population of corrected CD34$^+$ HSPCs from P1. Black lines indicate deletions, and the short ticks represent insertions.

target locus at *CYBB* exon 7 was performed to determine rates of conversion to the normal sequence (repair), uncorrected mutated "T," and indels including sequencing errors (Fig. 5D and fig. S5). About 250,000 reads were obtained for each sample. The gene repair rate increased with the amount of ssODN used up to 200 to 300 µg/ml. However, at the higher amounts of ssODN, the percentage of indels decreased (fig. S5). Gene repair at the DNA level paralleled the appearance of gp91^{phox} protein expression in gene-corrected cells (Fig. 5B) and demonstrated the stability of gene repair for up to 20 weeks (Fig. 5B). By comparing the gene repair rates before and after transplant, we observed a maximum ~35% decrease in gene repair 20 weeks after transplant (Fig. 5C). The frequencies of repaired alleles in corrected P1 CD34$^+$ HSPCs before transplant and in human CD45$^+$ myeloid cells in mouse bone marrow at 8, 16, or 20 weeks after transplant were compared. Consistent levels of gene correction up to 20 weeks after transplant were observed (Fig. 5C). Notably, when the FACS-sorted human CD45$^+$ cells were cultured in vitro for 3 weeks, the frequency of gene-repaired alleles remained unchanged, demonstrating that there was no relative survival advantage for gene-repaired cells (Fig. 3C). Similarly, the percentage of repaired alleles in gene-corrected P1 CD34$^+$ HSPCs remained stable after 3 to 4 weeks of differentiation into myeloid cells in vitro (Fig. 3D).

The same CRISPR-mediated approach and amount of ssODN were used to correct CD34$^+$ HSPCs from patient 2 (P2). Whereas gene repair rates could be achieved in a similar range to P1 (fig. S6), additional optimization was necessary. The repair rate showed a less than 50% decrease after transplant of gene-corrected P2 CD34$^+$ HSPCs into NSG mice. Our data from the two X-CGD patients highlighted that efficient CRISPR-mediated gene repair is, in principle, possible, but careful validation of the conditions is necessary to achieve consistent optimal results. We observed toxicities when using higher amounts (300 to 400 µg/ml) of ssODN, which resulted in lower efficiencies of gene repair in vitro (8 to 9%) and only 2 to 4% of human CD45$^+$ cells in mouse bone marrow expressing gp91^{phox} protein at 26 weeks after transplant (fig. S7). Despite the low in vitro gene repair rates, genetic analysis of the FACS-sorted gp91^{phox}-expressing human CD20$^+$ B cells from mouse spleen at 26 weeks after transplant of CRISPR-treated P2 CD34$^+$ HSPCs confirmed the presence of the repaired sequence in 56 to 59% of alleles compared to 0% in uncorrected P2 CD34$^+$ HSPCs (table S1). In FACS-sorted P2 CD34$^+$ HSPCs from mouse bone marrow, evidence of gene-corrected alleles was found in up to 0.3% of these cells (0.1 to 0.3%) compared to 95% of healthy control CD34$^+$ HSPCs. Together, these data demonstrate long-term persistence (≤26 weeks) of gene correction

in CD34$^+$ HSPCs, myeloid cells, and lymphoid cells in mouse bone marrow after transplant.

Specificity of CRISPR-mediated gene repair in CD34$^+$ HSPCs from X-CGD patients

Off-target cutting is a major concern for the clinical application of CRISPR-mediated gene repair and may vary between different guide sequences. To assess the specificity of the single-guide RNA used here, we treated healthy control CD34$^+$ HSPCs with the CRISPR/single-guide RNA targeting the C676T mutation in exon 7 of the *CYBB* gene. Despite only one base pair mismatch, the indel rate dropped ~30-fold, thus confirming the specificity of the single-guide RNA for the *CYBB* exon 7 C676T mutation (fig. S8 and table S4). All of the computationally predicted possible alternate target sites (http://crispr.cos.uni-heidelberg.de) based on homology to the single-guide RNA had >3 to 4 base pair (bp) mismatches. We performed targeted sequencing of seven such targets for further study (table S2). Polymerase chain reaction (PCR) primers specific for each predicted off-target region were used to amplify DNA from CRISPR/single-guide RNA–corrected P1 CD34$^+$ HSPCs and uncorrected healthy control CD34$^+$ HSPCs. At a read depth of up to 10,000×, we did not detect any indels that would have been indicative of CRISPR cutting and NHEJ repair. The indels were likely to be 5 to 15 bp, as shown by targeted Sanger sequencing at the *CYBB* locus (Fig. 6). At a read depth of 1,200,000×, we observed one single indel (>3 bp) at the *RP11-454H19.2* gene in the CRISPR-corrected P1 CD34$^+$ HSPCs (table S2). However, we also observed one single indel in the uncorrected healthy control CD34$^+$ HSPCs, indicating that this could be due to amplification/sequencing errors at this level of coverage. Whole-exome sequencing at 800× coverage of corrected patient CD34$^+$ HSPCs also failed to detect any off-target indels. We performed necropsy of NSG mice transplanted with corrected CD34$^+$ HSPCs at 20 weeks after transplant and confirmed the absence of tumors.

DISCUSSION

Gene therapy for the treatment of genetic disorders of the hematopoietic system relies on efficient and safe correction of autologous CD34$^+$ HSPCs derived from bone marrow or peripheral blood after mobilization with G-CSF. Despite advances in the development of nucleases enabling gene editing to create a wide range of genetically modified animals and plants, CD34$^+$ HSPCs have appeared to be resistant to HDR-mediated gene modification. Here, we show that CRISPR/single-guide RNA can be delivered efficiently into CD34$^+$ HSPCs with low toxicities using a scalable electroporation system. The optimized CRISPR methodology converted a single base pair mutation to the normal sequence, thereby restoring function to the gp91^{phox} protein encoded by the *CYBB* gene, which remained under the control of its endogenous promoter. The endogenously regulated expression of gp91^{phox} avoided concerns regarding ectopic expression of gp91^{phox} that have led to the use of a myeloid-specific promoter for lentiviral gene therapy for treating CGD (*28*). Cell type– and developmental stage–appropriate regulation of gp91^{phox} may partly contribute to the improved engraftment of patient CD34$^+$ HSPCs obtained here, although further studies will be required to determine whether NOX2 expression during engraftment could be detrimental. Other specific engraftment capabilities of CRISPR-corrected CD34$^+$ HSPCs will be a focus of future studies.

Reduced toxicities associated with CRISPR-mediated correction of patient CD34$^+$ HSPCs may also contribute to the engraftment rates observed in this study. Our data demonstrated similar rates of HDR gene repair in the various CD34$^+$ HSPC subpopulations, as observed in primitive CD34$^+$CD133$^+$CD90$^+$ progenitor cells. Gene repair in the latter cells resulted in functional restoration of gp91^{phox} in myeloid and lymphoid progenies at clinically relevant levels, as detected in the peripheral blood of NSG mice up to 20 weeks after transplant, with sequence-confirmed repair evident for up to 6.5 months. Previous work with zinc finger nuclease mRNA and integration-deficient lentiviral vector donor co-delivery to CD34$^+$ HSPCs from either human cord blood or bone marrow achieved ~3 to 11% gene targeting efficiency in vitro, which decreased to ~1% after transplant into immunodeficient mice (*15*, *16*). Similarly, HDR gene editing in peripheral blood CD34$^+$ HSPCs by co-delivery of mega-TAL nuclease and a single-stranded rAAV (recombinant adeno-associated virus) donor template achieved comparable levels of ~14% allele correction frequencies in vitro.

The limitations of this study are several-fold. First, there are few CGD patients for whom sufficient numbers of CD34$^+$ HSPCs are available for research purposes. Although we could successfully correct CD34$^+$ HSPCs from two separate patients with the *CYBB* exon 7 C676T mutation, long-term studies with additional patient HSPCs and larger numbers of mice will be required. For example, secondary and tertiary transplants of bone marrow from NSG mouse recipients of corrected CD34$^+$ HSPCs may be required to confirm that CD34$^+$ pluripotent stem cells were corrected and to ensure the absence of unwanted potentially oncogenic mutations or other unexpected changes. Nevertheless, gene correction in FACS-sorted CD34$^+$CD133$^+$CD90$^+$ cells in vitro and in both human myeloid and lymphoid cells in mouse blood after transplant of corrected CD34$^+$ HSPCs suggests that primitive stem cells were repaired. Second, our success at correction of this single, albeit most common, mutation in X-CGD may not extend to other mutations. Third, we may have missed detection of potentially deleterious mutations not present in whole exomes or at predicted sites. Although a search for off-target cuts failed to identify any, nevertheless, given that the specificity and off-target cut rates will likely vary depending on the specific mutation and single-guide RNA used, a careful evaluation of each set of CRISPR/Cas reagents before clinical application will be critical. Rapid innovations in the field may reduce such problems, for example, by using truncated single-guide RNAs and paired Cas9 nickases or modifying amino acids at Cas9–target DNA contact sites (*29*). Advances in modifications to the protospacer adjacent motif recognition site will also extend genomic sites accessible to this CRISPR/Cas9 approach (*30*, *31*). Finally, the level of gene correction in human cells circulating in mouse peripheral blood may not be predictive of correction of the human disease. On the basis of clinical outcomes in lyonized female carriers of X-CGD with skewed X chromosome inactivation, resulting in variable numbers of cells with functional NOX2 activity, and the observation that improvements in outcome in X-CGD arise from incrementally increased residual NOX2 function (*17*), we believe that gene repair resulting in ~15% of circulating neutrophils having normal NOX2 function would result in a reduction in infections and improved outcomes in patients. This provides a strong rationale for a CRISPR-mediated gene mutation repair approach for treating CGD.

CRISPR/oligonucleotide-mediated gene editing of CD34$^+$ HSPCs for other CGD mutations will require optimization and off-target evaluation for each set of guide RNAs. Nevertheless, this study provides a proof of principle demonstrating the feasibility of a CRISPR-targeted approach for gene mutation repair in a monogenic blood disorder, resulting in restoration of endogenously regulated gene expression

and protein function. This approach is potentially applicable to more common diseases attributable to single base pair mutations such as sickle cell anemia (*15*).

MATERIALS AND METHODS

Study design

The goal of our study was to develop a CRISPR approach to repair a *CYBB* gene mutation in CD34$^+$ HSPCs from patients with X-CGD and achieve clinically relevant protein expression after transplant into NSG immunodeficient mice. The *CYBB* exon 7 C676T mutation results in the loss of gp91^{phox} expression and NOX2 function in myeloid cells. Optimization of the CRISPR approach was conducted in patient-derived EBV-transformed B cell lines, and selected conditions were applied to CD34$^+$ HSPCs from two X-CGD patients. Evaluation of gene repair included sequencing, FACS analysis for gp91^{phox} expression, assessment of NOX2-dependent superoxide radical production, and antibactericidal activity of in vitro or in vivo differentiated myeloid cells; comparisons were made to healthy control CD34$^+$ HSPCs.

CD34$^+$ HSPCs from two X-CGD patients were treated with varying doses of ssODN before transplantation into NSG mice (three mice per group) to determine the effects of ssODN on engraftment and gene repair rates. The same experiment was repeated two additional times. Analysis was conducted at various time points after transplant to assess sustainability of gene correction in vivo. Analysis of gene correction was performed on patient CD34$^+$ HSPCs before and after transplant to assess efficacy of gene repair. Potential off-target CRISPR cut sites were identified by an algorithm and sequenced. Whole-exome sequencing was also performed to identify other genome alterations.

Human blood cells

CD34$^+$ HSPCs were obtained after written informed consent under the auspices of the NIAID Institutional Review Board–approved protocols 05-I-0213 and 94-I-0073. The conduct of these studies conformed to the Declaration of Helsinki protocols and all U.S. federal regulations required for the protection of human subjects. Healthy donors and patients with X-CGD underwent leukapheresis after CD34$^+$ HSPC mobilization with G-CSF (15 μg/kg daily) for 5 days and plerixafor at 12 hours before blood collection.

Mouse studies

Use of immunodeficient NOD.Cg-Prkdcscid Il2rgtm1Wjl/SzJ (NSG) mice (The Jackson Laboratory) for xenotransplant studies was approved by the NIAID Institutional Animal Care and Use Committee under animal use protocol LHD 3E. The conduct of these studies conformed to Association for Assessment and Accreditation of Laboratory Animal Care International guidelines and all U.S. federal regulations governing the protection of research animals.

CRISPR/Cas9 mRNA, single-guide RNA, and single-stranded oligonucleotide donor

Cas9 plasmid for double-stranded DNA cuts and the single-guide RNA were purchased from the Genome Engineering Center, Washington University, St. Louis. The template for in vitro RNA transcription was obtained by linearization of the Cas9 plasmid with Xho I. A number of single-guide RNAs were evaluated (fig. S1). The single-guide RNA template was made by PCR amplification with primers conjugated with T7 promoter for the forward primer and shared common reverse primer: gRNA1.F, 5′-TTAATACGACTCACTATAGGTTTCCTATTACTAAATGATC; gRNA2.F, 5′-TTAATACGACTCACTATAGGCACCCAGATGAATTGTACGT; gRNA3.F, 5′-TTAATACGACTCACTATAGGTGCCCACGTACAATTCATCT; gRNA8.F, 5′-TTAATACGACTCACTATAGGAGTCCAGATCATTTAGTAAT; reverse primer, 5′-AAAAGCACCGACTCGGTGCC-3′.

The mRNA for Cas9 and single-guide RNA was made by mMESSAGE mMACHINE T7 ULTRA Transcription Kit (Ambion). Chemically modified ssODN was purchased from Integrated DNA Technologies, with the following sequence for single-guide RNA2: 5′-CTATTACTAAATGATCTGGACTTACATTTTTCACCCAGACGAATTGTACGTGGGCAGACCGCAGAGAGTTTGGCTGTGCATAATATAACAGTTTGTGAAC-3′.

In vitro CD34$^+$ HSPCs and immortalized B cell lines

Human CD34$^+$ HSPCs were cultured in complete medium consisting of StemSpan SFEM (STEMCELL Technologies Inc.), supplemented with stem cell factor, fms-related tyrosine kinase 3 ligand, and thrombopoietin, each at 100 ng/ml (PeproTech). Peripheral blood mononuclear cells from a patient with X-CGD caused by a *CYBB* exon 7 C676T mutation were used to establish an EBV-transformed B cell line for preliminary evaluation of reagents. This cell line from P1 was cultured in RPMI 1640 (Lonza) supplemented with 20% fetal calf serum (FCS) (HyClone) and 2 mM glutamine at a density of 1 million to 2 million cells/ml.

Cell viability was determined by FACS analysis on the basis of forward scatter/side scatter dot plot and verified by exclusion of propidium iodide. The relative viable cell number was determined by timed collection of events by FACS. A standardized correlation curve was determined by the cell number obtained by FACS versus the number enumerated by hemocytometer, with the intercept set at 0. Cell number in samples was determined by a FACS timed collection multiplied by the dilution factor.

For myeloid cell differentiation, CD34$^+$ HSPCs were cultured in Dulbecco's modified Eagle's medium supplemented with 20% FCS and G-CSF (100 ng/ml). Fresh medium was provided every 3 to 4 days.

Electroporation

Cryopreserved HSPCs were thawed (day 0) and then cultured in complete medium (described above). On day 2, cells were counted and resuspended in electroporation buffer (MaxCyte Systems) at 2×10^7 to 5×10^7/ml. For most experiments, in vitro transcribed CRISPR/Cas9 nuclease RNA (100 μg/ml), single-guide RNA (200 μg/ml), and single-stranded oligonucleotide (ssODN) (up to 300 μg/ml) were added as indicated and electroporated per the manufacturer's specifications. Conditions using higher amounts of single-guide RNA (300 μg/ml) and ssODN (400 μg/ml) were also tested. After electroporation, cells were incubated at 37°C for 20 min before transfer to complete medium for culture.

Flow cytometry for gp91^{phox} and DHR assay

Human hematopoietic cells were detected with anti-human CD45-phycoerythrin, and human gp91^{phox} expression was determined by indirect staining with murine monoclonal antibody 7D5, followed by FITC-conjugated goat anti-mouse immunoglobulin G antibody. For flow cytometric analysis, FACS (argon laser, Becton Dickinson) was used.

Chemiluminescence

Cells (100,000) in Hanks' balanced salt solution and luminol (100 mM) were added into the wells of a 96-well polypropylene flat-bottom,

chimney well microplate (Greiner Bio-One). The plate was wrapped in foil to protect from light and incubated at 37°C for 10 min. PMA (100 ng/ml) was added to triplicate wells containing cells and luminol. The microplate was read immediately with a luminometer at 37°C for 120 min to assess ROS production by chemiluminescence.

Bactericidal assay

Myeloid-differentiated cells were washed three times in phenol red–free RPMI containing L-glutamine (Invitrogen) to remove antibiotics present during previous culture. *G. bethesdensis* cultures were prepared, and killing assays were conducted as previously described (*21*), with some modifications. Briefly, *G. bethesdensis* was preopsonized with human serum, washed, and then cultured with cells in medium containing 10% fetal bovine serum (Invitrogen) at an MOI of 1. After 24 hours, cells were lysed with 0.5% saponin and mechanically sheared with a syringe. Lysates were dilution-plated, and CFU were enumerated after 3 to 4 days of incubation at 37°C.

Surveyor Nuclease assay (Cel-1 assay)

With Surveyor Nuclease for recognition and cleavage of mismatches, amplified products using the primers below allowed determination of cleavage activity at target sites used per the manufacturer's instructions (Integrated DNA Technologies). PCR primers for amplification of genomic DNA relevant to detect gene integration/correction are as follows: Cel.F, 5′-GCACAAAGGCACTGTAGGGGCCAGC-3′; Cel. R, 5′-TGCTGGTATCTGAAGAGGCCCTTTGC-3′.

Transplantation of CD34$^+$ HSPCs into NSG mice

Six- to 8-week-old NSG mice were given busulfan (20 mg/kg) via intraperitoneal injections 24 hours before transplant. Mice received 1 million to 3 million human cells via tail vein injection. After busulfan treatment, NSG mice received neomycin-supplemented water for prophylaxis.

Human CD45$^+$ cell isolation and genomic DNA extraction

Bone marrow cells flushed from NSG femurs were subjected to human CD45 bead selection (Dynabeads). Genomic DNA was extracted using the DNeasy Blood and Tissue Kit (Qiagen).

Next-generation sequencing

The on-target repair efficiency and indel frequencies were determined using Illumina MiSeq. Genomic DNA (1 μg), equivalent to 160,000 cells, was used to estimate the extent of repair. We amplified a 276-bp region around the CRISPR target (*CYBB* exon 7) with a pair of primers outside the donor DNA region (forward primer, 5′-TTCAGAGGGAGCAATAAGCTAT-3′; reverse primer, 5′-CATACCATAGGAGGGTTTCCAG-3′), with Illumina adaptors and barcodes, and then sequenced the amplicon with the Illumina 2 × 250 bp paired-end sequencing kit on MiSeq. Generally, 0.25 million to 0.5 million reads were generated for each sample to quantify the frequency of normal and mutant alleles.

To determine the rate of off-target indels, deep exome sequencing at 800× coverage was performed. Human Agilent SureSelect Target Enrichment Kit V5 (Agilent) was used for library construction, and the Illumina NextSeq was used for sequencing with 2 × 150 bp paired-end reads. Sequence reads were aligned and analyzed using Illumina BaseSpace Apps. Indels were identified and categorized, confirming on-target indels near *CYBB* target site without any other indels across the genome at 800× coverage for the CRISPR-treated samples.

Statistical analyses

Statistical testing was performed using GraphPad Prism for Macintosh (version 7.0). For data pertaining to different doses of oligonucleotides used in gene correction, an ordinary one-way analysis of variance (ANOVA) was performed with Tukey's multiple comparisons test.

SUPPLEMENTARY MATERIALS

www.sciencetranslationalmedicine.org/cgi/content/full/9/372/eaah3480/DC1

Fig. S1. Evaluation of the CRISPR/Cas9 system in an immortalized B cell line from a patient with the *CYBB* exon 7 C676T mutation.

Fig. S2. Effects of phosphorothioate modifications to a single-stranded oligonucleotide donor template for CRISPR-mediated gene repair in immortalized B cells derived from an X-CGD patient.

Fig. S3. Optimization of CRISPR/Cas9/single-guide RNA and single-stranded oligonucleotide delivery into human CD34$^+$ HSPCs by electroporation.

Fig. S4. FACS analysis for gp91^{phox} expression in CD3$^+$ T cells.

Fig. S5. Sequencing of *CYBB* exon 7 in FACS-sorted human CD45$^+$ cells derived from P1 CD34$^+$ HSPCs after transplant into NSG mice.

Fig. S6. CRISPR-mediated correction of CD34$^+$ HSPCs from a second X-CGD patient (P2).

Fig. S7. Peripheral blood from NSG mice 26 weeks after transplant with corrected P2 CD34$^+$ HSPCs.

Fig. S8. Specificity of CRISPR/single-guide RNA for targeting the *CYBB* mutation.

Table S1. Deep sequencing of *CYBB* site in sorted human CD45$^+$CD34$^+$ cells from the bone marrow and spleen of NSG mice at 6.5 months after transplant of gene-corrected P2 CD34$^+$ HSPCs.

Table S2. Potential alternate genomic target sites.

Table S3. Targeted sequencing of selected computationally predicted off-target sites.

Table S4. Evaluation of specificity of CRISPR/single-guide RNA by sequencing CD34$^+$ HSPCs from healthy donors and two X-CGD patients using the same mutation-specific single-guide RNA2.

REFERENCES AND NOTES

1. C. C. Dvorak, A. Hassan, M. A. Slatter, M. Hönig, A. C. Lankester, R. H. Buckley, M. A. Pulsipher, J. H. Davis, T. Güngör, M. Gabriel, J. H. Bleesing, N. Bunin, P. Sedlacek, J. A. Connelly, D. F. Crawford, L. D. Notarangelo, S.-Y. Pai, J. Hassid, P. Veys, A. R. Gennery, M. J. Cowan, Comparison of outcomes of hematopoietic stem cell transplantation without chemotherapy conditioning by using matched sibling and unrelated donors for treatment of severe combined immunodeficiency. *J. Allergy Clin. Immunol.* **134**, 935–943. e15 (2014).
2. M. G. Ott, M. Schmidt, K. Schwarzwaelder, S. Stein, U. Siler, U. Koehl, H. Glimm, K. Kühlcke, A. Schilz, H. Kunkel, S. Naundorf, A. Brinkmann, A. Deichmann, M. Fischer, C. Ball, I. Pilz, C. Dunbar, Y. Du, N. A. Jenkins, N. G. Copeland, U. Lüthi, M. Hassan, A. J. Thrasher, D. Hoelzer, C. von Kalle, R. Seger, M. Grez, Correction of X-linked chronic granulomatous disease by gene therapy, augmented by insertional activation of *MDS1-EVI1*, *PRDM16* or *SETBP1*. *Nat. Med.* **12**, 401–409 (2006).
3. K. Boztug, M. Schmidt, A. Schwarzer, P. P. Banerjee, I. A. Díez, R. A. Dewey, M. Böhm, A. Nowrouzi, C. R. Ball, H. Glimm, S. Naundorf, K. Kühlcke, R. Blasczyk, I. Kondratenko, L. Maródi, J. S. Orange, C. von Kalle, C. Klein, Stem-cell gene therapy for the Wiskott–Aldrich syndrome. *N. Engl. J. Med.* **363**, 1918–1927 (2010).
4. H. T. Lin, H. Masaki, T. Yamaguchi, T. Wada, A. Yachie, K. Nishimura, M. Ohtaka, M. Nakanishi, H. Nakauchi, M. Otsu, An assessment of the effects of ectopic gp91^{phox} expression in XCGD iPSC-derived neutrophils. *Mol. Ther. Methods Clin. Dev.* **2**, 15046 (2015).
5. S. S. De Ravin, X. Wu, S. Moir, S. Anaya-O'Brien, N. Kwatemaa, P. Littel, N. Theobald, U. Choi, L. Su, M. Marquesen, D. Hilligoss, J. Lee, C. M. Buckner, K. A. Zarember, G. O'Connor, D. McVicar, D. Kuhns, R. E. Throm, S. Zhou, L. D. Notarangelo, I. C. Hanson, M. J. Cowan, E. Kang, C. Hadigan, M. Meagher, J. T. Gray, B. P. Sorrentino, H. L. Malech, Lentiviral hematopoietic stem cell gene therapy for X-linked severe combined immunodeficiency. *Sci. Transl. Med.* **8**, 335ra57 (2016).
6. A. Biffi, E. Montini, L. Lorioli, M. Cesani, F. Fumagalli, T. Plati, C. Baldoli, S. Martino, A. Calabria, S. Canale, F. Benedicenti, G. Vallanti, L. Biasco, S. Leo, N. Kabbara, G. Zanetti, W. B. Rizzo, N. A. L. Mehta, M. P. Cicalese, M. Casiraghi, J. J. Boelens, U. Del Carro, D. J. Dow, M. Schmidt, A. Assanelli, V. Neduva, C. Di Serio, E. Stupka, J. Gardner, C. von Kalle, C. Bordignon, F. Ciceri, A. Rovelli, M. G. Roncarolo, A. Aiuti, M. Sessa, L. Naldini, Lentiviral hematopoietic stem cell gene therapy benefits metachromatic leukodystrophy. *Science* **341**, 1233158 (2013).
7. A. Aiuti, L. Biasco, S. Scaramuzza, F. Ferrua, M. P. Cicalese, C. Baricordi, F. Dionisio, A. Calabria, S. Giannelli, M. C. Castiello, M. Bosticardo, C. Evangelio, A. Assanelli,

M. Casiraghi, S. Di Nunzio, L. Callegaro, C. Benati, P. Rizzardi, D. Pellin, C. Di Serio, M. Schmidt, C. Von Kalle, J. Gardner, N. Mehta, V. Neduva, D. J. Dow, A. Galy, R. Miniero, A. Finocchi, A. Metin, P. P. Banerjee, J. S. Orange, S. Galimberti, M. G. Valsecchi, A. Biffi, E. Montini, A. Villa, F. Ciceri, M. G. Roncarolo, L. Naldini, Lentiviral hematopoietic stem cell gene therapy in patients with Wiskott-Aldrich syndrome. *Science* **341**, 1233151 (2013).
8. G. Santilli, A. J. Thrasher, Patching up hematopoietic stem cells. *Nat. Biotechnol.* **33**, 1236–1238 (2015).
9. M. Jinek, K. Chylinski, I. Fonfara, M. Hauer, J. A. Doudna, E. Charpentier, A programmable dual-RNA–guided DNA endonuclease in adaptive bacterial immunity. *Science* **337**, 816–821 (2012).
10. P. Mali, K. M. Esvelt, G. M. Church, Cas9 as a versatile tool for engineering biology. *Nat. Methods* **10**, 957–963 (2013).
11. L. Cong, F. A. Ran, D. Cox, S. Lin, R. Barretto, N. Habib, P. D. Hsu, X. Wu, W. Jiang, L. A. Marraffini, F. Zhang, Multiplex genome engineering using CRISPR/Cas systems. *Science* **339**, 819–823 (2013).
12. Q. Shan, Y. Wang, J. Li, C. Gao, Genome editing in rice and wheat using the CRISPR/Cas system. *Nat. Protoc.* **9**, 2395–2410 (2014).
13. J. A. Doudna, E. Charpentier, Genome editing. The new frontier of genome engineering with CRISPR-Cas9. *Science* **346**, 1258096 (2014).
14. J. A. Doudna, E. J. Sontheimer, Eds., *The Use of CRISPR/Cas9, ZFNs, and TALENs in Generating Site-Specific Genome Alterations,* vol. 546 of *Methods in Enzymology* (Academic Press, 2014), pp. xix–xx.
15. M. D. Hoban, G. J. Cost, M. C. Mendel, Z. Romero, M. L. Kaufman, A. V. Joglekar, M. Ho, D. Lumaquin, D. Gray, G. R. Lill, A. R. Cooper, F. Urbinati, S. Senadheera, A. Zhu, P.-Q. Liu, D. E. Paschon, L. Zhang, E. J. Rebar, A. Wilber, X. Wang, P. D. Gregory, M. C. Holmes, A. Reik, R. P. Hollis, D. B. Kohn, Correction of the sickle cell disease mutation in human hematopoietic stem/progenitor cells. *Blood* **125**, 2597–2604 (2015).
16. P. Genovese, G. Schiroli, G. Escobar, T. Di Tomaso, C. Firrito, A. Calabria, D. Moi, R. Mazzieri, C. Bonini, M. C. Holmes, P. D. Gregory, M. van der Burg, B. Gentner, E. Montini, A. Lombardo, L. Naldini, Targeted genome editing in human repopulating haematopoietic stem cells. *Nature* **510**, 235–240 (2014).
17. D. B. Kuhns, W. G. Alvord, T. Heller, J. J. Feld, K. M. Pike, B. E. Marciano, G. Uzel, S. S. DeRavin, D. A. Priel, B. P. Soule, K. A. Zarember, H. L. Malech, S. M. Holland, J. I. Gallin, Residual NADPH oxidase and survival in chronic granulomatous disease. *N. Engl. J. Med.* **363**, 2600–2610 (2010).
18. A. C. Battersby, C. M. Cale, D. Goldblatt, A. R. Gennery, Clinical manifestations of disease in X-linked carriers of chronic granulomatous disease. *J. Clin. Immunol.* **33**, 1276–1284 (2013).
19. R. Flynn, A. Grundmann, P. Renz, W. Hänseler, W. S. James, S. A. Cowley, M. D. Moore, CRISPR-mediated genotypic and phenotypic correction of a chronic granulomatous disease mutation in human iPS cells. *Exp. Hematol.* **43**, 838–848.e3 (2015).
20. F. Chen, S. M. Pruett-Miller, G. D. Davis, Gene editing using ssODNs with engineered endonucleases. *Methods Mol. Biol.* **1239**, 251–265 (2015).
21. X. Rios, A. W. Briggs, D. Christodoulou, J. M. Gorham, J. G. Seidman, G. M. Church, Stable gene targeting in human cells using single-strand oligonucleotides with modified bases. *PLOS ONE* **7**, e36697 (2012).
22. I. Papaioannou, P. Disterer, J. S. Owen, Use of internally nuclease-protected single-strand DNA oligonucleotides and silencing of the mismatch repair protein, MSH2, enhances the replication of corrected cells following gene editing. *J. Gene Med.* **11**, 267–274 (2009).
23. S. R. Panch, Y. Y. Yau, E. M. Kang, S. S. De Ravin, H. L. Malech, S. F. Leitman, Mobilization characteristics and strategies to improve hematopoietic progenitor cell mobilization and collection in patients with chronic granulomatous disease and severe combined immunodeficiency. *Transfusion* **55**, 265–274 (2015).
24. K. A. Zarember, K. R. Marshall-Batty, A. R. Cruz, J. Chu, M. E. Fenster, A. R. Shoffner, L. S. Rogge, A. R. Whitney, M. Czapiga, H. H. Song, P. A. Shaw, K. Nagashima, H. L. Malech, F. R. DeLeo, S. M. Holland, J. I. Gallin, D. E. Greenberg, Innate immunity against *Granulibacter bethesdensis*, an emerging Gram-negative bacterial pathogen. *Infect. Immun.* **80**, 975–981 (2012).
25. S. Moir, S. S. De Ravin, B. H. Santich, J. Y. Kim, J. G. Posada, J. Ho, C. M. Buckner, W. Wang, L. Kardava, M. Garofalo, B. E. Marciano, J. Manischewitz, L. R. King, S. Khurana, T.-W. Chun, H. Golding, A. S. Fauci, H. L. Malech, Humans with chronic granulomatous disease maintain humoral immunologic memory despite low frequencies of circulating memory B cells. *Blood* **120**, 4850–4858 (2012).
26. M. Bertolotti, G. Farinelli, M. Galli, A. Aiuti, R. Sitia, AQP8 transports NOX2-generated H_2O_2 across the plasma membrane to promote signaling in B cells. J. Leukoc. Biol. **100**, 1071–1079 (2016).
27. M. Chiriaco, G. Farinelli, V. Capo, E. Zonari, S. Scaramuzza, G. Di Matteo, L. S. Sergi, M. Migliavacca, R. J. Hernandez, F. Bombelli, E. Giorda, A. Kajaste-Rudnitski, D. Trono, M. Grez, P. Rossi, A. Finocchi, L. Naldini, B. Gentner, A. Aiuti, Dual-regulated lentiviral vector for gene therapy of X-linked chronic granulomatosis. *Mol. Ther.* **22**, 1472–1483 (2014).
28. G. Santilli, E. Almarza, C. Brendel, U. Choi, C. Beilin, M. P. Blundell, S. Haria, K. L. Parsley, C. Kinnon, H. L. Malech, J. A. Bueren, M. Grez, A. J. Thrasher, Biochemical correction of X-CGD by a novel chimeric promoter regulating high levels of transgene expression in myeloid cells. *Mol. Ther.* **19**, 122–132 (2011).
29. B. P. Kleinstiver, V. Pattanayak, M. S. Prew, S. Q. Tsai, N. T. Nguyen, Z. Zheng, J. K. Joung, High-fidelity CRISPR–Cas9 nucleases with no detectable genome-wide off-target effects. *Nature* **529**, 490–495 (2016).
30. B. P. Kleinstiver, M. S. Prew, S. Q. Tsai, N. T. Nguyen, V. V. Topkar, Z. Zheng, J. K. Joung, Broadening the targeting range of *Staphylococcus aureus* CRISPR-Cas9 by modifying PAM recognition. *Nat. Biotechnol.* **33**, 1293–1298 (2015).
31. B. P. Kleinstiver, M. S. Prew, S. Q. Tsai, V. V. Topkar, N. T. Nguyen, Z. Zheng, A. P. W. Gonzales, Z. Li, R. T. Peterson, J.-R.J. Yeh, M. J. Aryee, J. K. Joung, Engineered CRISPR-Cas9 nucleases with altered PAM specificities. *Nature* **523**, 481–485 (2015).

Acknowledgments: We thank the patients for their contribution to this study. We thank S. Miller in the Genome Engineering Center, Washington University, St. Louis, for the design of the guide RNAs and scientific discussions about CRISPR/Cas9 technology. We also thank the clinical support staff in the Laboratory of Host Defenses for their provision of clinical care and patient resources. We also thank the Department of Transfusion Medicine at the NIH Clinical Center for their collection and processing of $CD34^+$ cells from patients and healthy donors. **Funding:** This research was supported by the Intramural Research Program of NIAID, NIH (Intramural project numbers Z01-A1-00644 and Z01-A1-00988) and the Maryland Stem Cell Research Fund (#2015-MSCRFP-1752). **Author contributions:** S.S.D.R., L.L., X.W., U.C., C.A., S.K., J.L., N.T.-W., J.C., L.K., A.V., P.N., and L.S. designed and/or performed all experiments. S.S.D.R., L.L., U.C., S.M., C.S., D.K., K.A.Z., M.V.P., and H.L.M. analyzed data, and M.G. organized human material. S.S.D.R., X.W., K.A.Z., and H.L.M. wrote and reviewed the paper. M.V.P. and H.L.M. provided funding. **Competing interests:** L.L., C.A., A.V., P.N., and M.V.P. are full-time employees of MaxCyte Biosystems. L.L. and M.V.P. are co-inventors of patent #PCT/US2015/025523, "Methods and compositions for modifying genomic DNA." The other authors declare that they have no competing interests. **Data and materials availability:** All necessary information for reagents is provided in the article. Deidentified cell lines can be provided upon request. The MaxCyte electroporator is used under a licensing agreement. MaxCyte has intellectual property and proprietary cell engineering platform technology that is supported by a U.S. Food and Drug Administration Master File. This technology is only available under a licensing agreement with MaxCyte.

Submitted 13 June 2016
Resubmitted 9 September 2016
Accepted 17 August 2016
Published 11 January 2017
10.1126/scitranslmed.aah3480

Citation: S. S. De Ravin, L. Li, X. Wu, U. Choi, C. Allen, S. Koontz, J. Lee, N. Theobald-Whiting, J. Chu, M. Garofalo, C. Sweeney, L. Kardava, S. Moir, A. Viley, P. Natarajan, L. Su, D. Kuhns, K. A. Zarember, M. V. Peshwa, H. L. Malech, CRISPR-Cas9 gene repair of hematopoietic stem cells from patients with X-linked chronic granulomatous disease. *Sci. Transl. Med.* **9**, eaah3480 (2017).

Science Translational Medicine

CRISPR-Cas9 gene repair of hematopoietic stem cells from patients with X-linked chronic granulomatous disease

Suk See De Ravin, Linhong Li, Xiaolin Wu, Uimook Choi, Cornell Allen, Sherry Koontz, Janet Lee, Narda Theobald-Whiting, Jessica Chu, Mary Garofalo, Colin Sweeney, Lela Kardava, Susan Moir, Angelia Viley, Pachai Natarajan, Ling Su, Douglas Kuhns, Kol A. Zarember, Madhusudan V. Peshwa and Harry L. Malech

Sci Transl Med **9**, eaah3480.
DOI: 10.1126/scitranslmed.aah3480

Seamless gene repair with CRISPR

Targeted gene therapy has been hampered by the inability to correct mutations in stem cells that can reconstitute the immune system after transplant into patients. De Ravin *et al*. now report that CRISPR, a DNA editing technology, corrected blood stem cells from patients with an immunodeficiency disorder (chronic granulomatous disease) caused by mutations in NOX2. CRISPR-repaired human stem cells engrafted in mice after transplant and differentiated into leukocytes with a functional NOX2 protein for up to 5 months. The authors did not detect off-target treatment effects, suggesting that this gene repair strategy may benefit patients with chronic granulomatous disease or other blood disorders.

Science Translational Medicine (ISSN 1946-6242) is published by the American Association for the Advancement of Science, 1200 New York Avenue NW, Washington, DC 20005. The title *Science Translational Medicine* is a registered trademark of AAAS.